iScience

CellPress
OPEN ACCESS

Article

Ablation of Ventral Midbrain/Pons GABA Neurons Induces Mania-like Behaviors with Altered Sleep Homeostasis and Dopamine D_2R-mediated Sleep Reduction

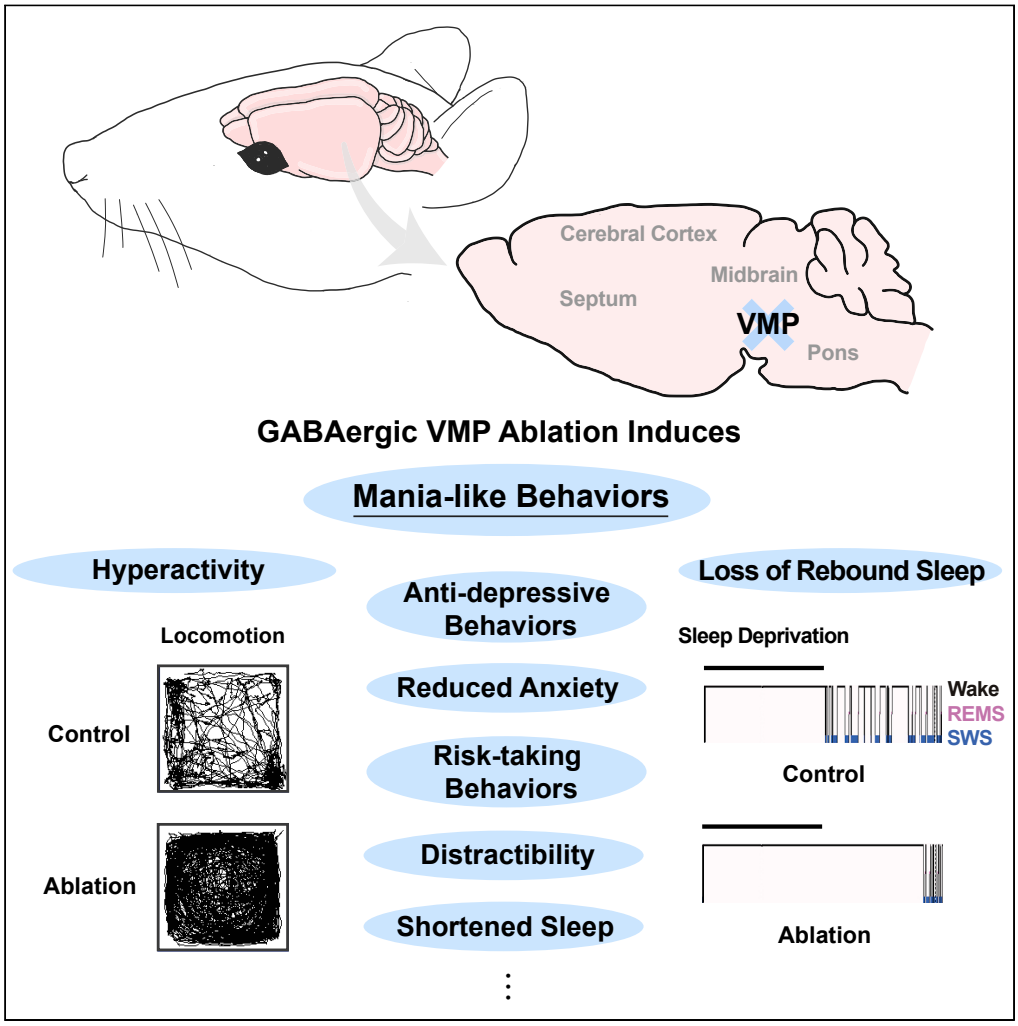

Takato Honda, Yohko Takata, Yoan Cherasse, ..., Masashi Yanagisawa, Michael Lazarus, Yo Oishi

takatoh@mit.edu (T.H.)
lazarus.michael.ka@u.tsukuba.ac.jp (M.L.)
oishi.yo.fu@u.tsukuba.ac.jp (Y.O.)

HIGHLIGHTS

Hyperactivity and anti-depressive behaviors are induced by loss of VMP GABA neurons

Homeostatic sleep rebound is lost together with largely shorten daily sleep

Dopamine D_2 receptors mediate the daytime sleep loss

Honda et al., iScience 23, 101240
June 26, 2020
https://doi.org/10.1016/j.isci.2020.101240

iScience

CellPress
OPEN ACCESS

Article

Ablation of Ventral Midbrain/Pons GABA Neurons Induces Mania-like Behaviors with Altered Sleep Homeostasis and Dopamine D_2R-mediated Sleep Reduction

Takato Honda,[1,2,*] Yohko Takata,[1] Yoan Cherasse,[1] Seiya Mizuno,[3] Fumihiro Sugiyama,[3] Satoru Takahashi,[1,3] Hiromasa Funato,[1,4] Masashi Yanagisawa,[1,5,6,7] Michael Lazarus,[1,*] and Yo Oishi[1,8,*]

SUMMARY

Individuals with the neuropsychiatric disorder mania exhibit hyperactivity, elevated mood, and a decreased need for sleep. The brain areas and neuronal populations involved in mania-like behaviors, however, have not been elucidated. In this study, we found that ablating the ventral medial midbrain/pons (VMP) GABAergic neurons induced mania-like behaviors in mice, including hyperactivity, anti-depressive behaviors, reduced anxiety, increased risk-taking behaviors, distractibility, and an extremely shortened sleep time. Strikingly, these mice also showed no rebound sleep after sleep deprivation, suggesting abnormal sleep homeostatic regulation. Dopamine D_2 receptor deficiency largely abolished the sleep reduction induced by ablating the VMP GABAergic neurons without affecting the hyperactivity and anti-depressive behaviors. Our data demonstrate that VMP GABAergic neurons are involved in the expression of mania-like behaviors, which can be segregated to the short-sleep and other phenotypes on the basis of the dopamine D_2 receptors.

INTRODUCTION

Sleep problems are the core components of mood disorders, such as bipolar disorder characterized by periods of depression and mania (Benca et al., 1997). The clinical criteria for mania include persistently elevated mood or energy and decreased need for sleep (American Psychiatric Association, 2013). In humans, infarctions of the midbrain or pontine areas induces secondary mania (Antelmi et al., 2014; Caplan, 2010; Drake et al., 1990; Satzer and Bond, 2016; Shen et al., 2005). In the present study, we focused on the ventral medial midbrain/pons (VMP) area, a region that contains sleep-regulating GABAergic neurons (Chowdhury et al., 2019; Takata et al., 2018; Yu et al., 2019). To elucidate the physiologic functions of VMP GABAergic neurons, we selectively ablated these neurons in mice with Cre-dependent viral expression of the diphtheria toxin subunit A (DTA) in the VMP of vesicular GABA transporter (VGAT; a marker of GABAergic neurons) Cre mice (VGAT-Cre$^{DTA/VMP}$ mice: Figures 1A and 1B). For controls, we prepared mice expressing humanized *Renilla reniformis*-derived green fluorescent protein (hrGFP) in the VMP GABAergic neurons (VGAT-Cre$^{hrGFP/VMP}$). These mice were subjected to a comprehensive behavioral test battery including various tasks that are reliably used to assess locomotor activity, depression-like behavior, sociability, anxiety, species-typical behavior, and learning and memory (Crawley, 2007; Crawley and Paylor, 1997).

RESULTS

GABAergic VMP Ablation Induces Hyperactivity, Anti-depressive Behaviors, and Reduced Anxiety

Our behavioral test battery revealed that VGAT-Cre$^{DTA/VMP}$ mice exhibited increased locomotor activity with a longer distance traveled in the open field test compared with control VGAT-Cre$^{hrGFP/VMP}$ mice ($p < 0.001$, Figure 1C). VGAT-Cre$^{DTA/VMP}$ mice also showed consistently decreased immobility in both the tail suspension test ($p < 0.01$, Figure 1D) and the forced swim test ($p < 0.0001$, Figure 1E), suggesting anti-depressive behaviors. In addition, VGAT-Cre$^{DTA/VMP}$ mice exhibited increased preference for the zone

[1]International Institute for Integrative Sleep Medicine (WPI-IIIS), University of Tsukuba, Tsukuba, Ibaraki 305-8575, Japan

[2]Department of Brain and Cognitive Sciences, Picower Institute for Learning and Memory, Massachusetts Institute of Technology (MIT), Cambridge, MA 02139, USA

[3]Laboratory Animal Resource Center and Trans-border Medical Research Center, University of Tsukuba, Tsukuba, Ibaraki 305-8575, Japan

[4]Department of Anatomy, Faculty of Medicine, Toho University, Ota, Tokyo 143-8540, Japan

[5]Department of Molecular Genetics, University of Texas Southwestern Medical Center, Dallas, TX 75390, USA

[6]Life Science Center for Survival Dynamics (TARA), University of Tsukuba, Tsukuba, Ibaraki 305-8575, Japan

[7]R&D Center for Frontiers of Mirai in Policy and Technology (F-MIRAI), University of Tsukuba, Tsukuba, Ibaraki 305-8575, Japan

[8]Lead Contact

*Correspondence: takatoh@mit.edu (T.H.), lazarus.michael.ka@u.tsukuba.ac.jp (M.L.), oishi.yo.fu@u.tsukuba.ac.jp (Y.O.)

https://doi.org/10.1016/j.isci.2020.101240

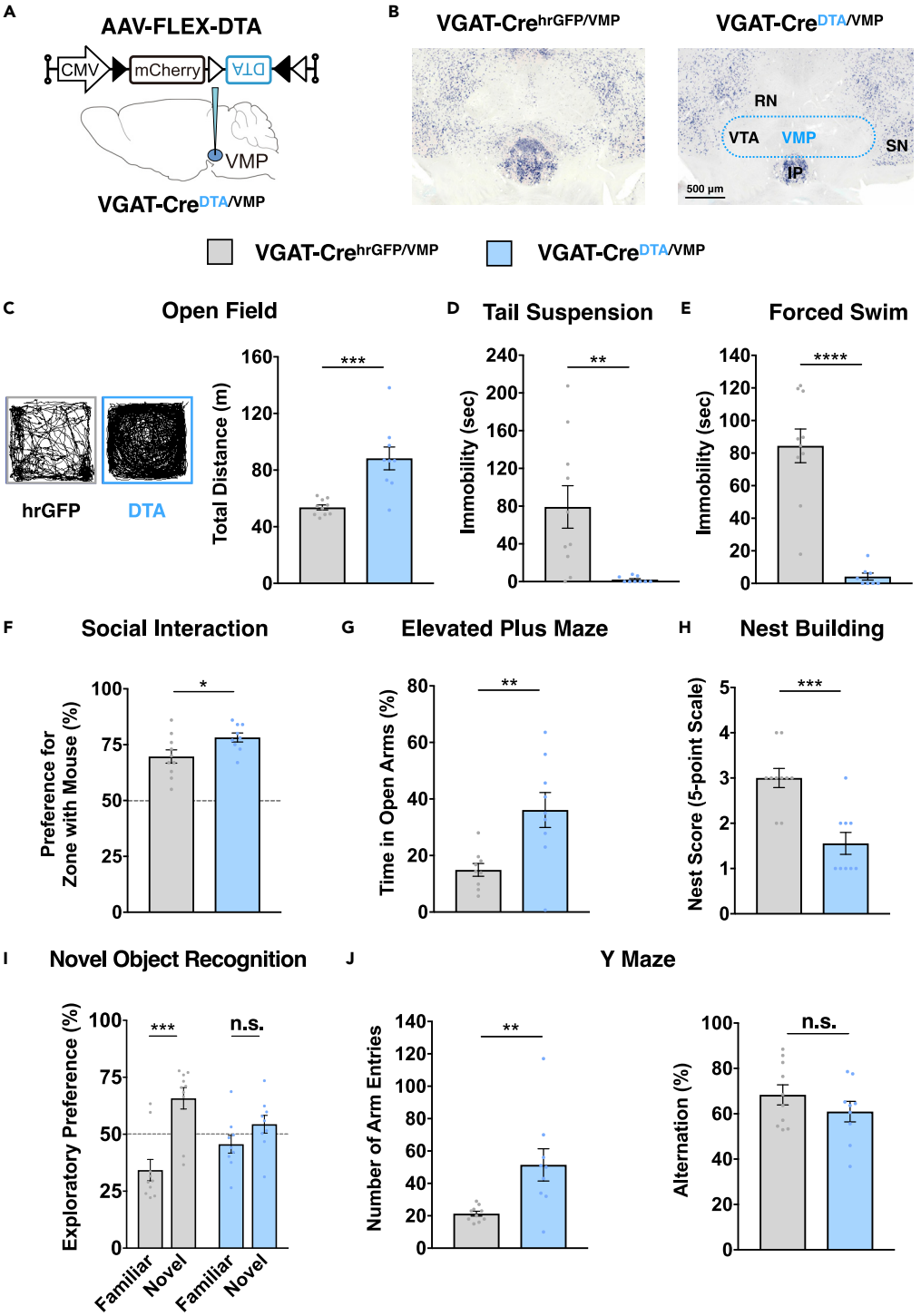

Figure 1. Selective Ablation of the VMP GABAergic Neurons Induces Hyperactivity, Anti-depressive Behaviors, and Reduced Anxiety

(A) VGAT-Cre mice were injected with AAV-FLEX-hrGFP (VGAT-Cre$^{hrGFP/VMP}$ mice; control) or AAV-FLEX-DTA (VGAT-Cre$^{DTA/VMP}$ mice) into the VMP region.

(B) Brain sections stained against VGAT mRNA. VMP GABAergic neurons were selectively ablated in VGAT-Cre$^{DTA/VMP}$ mice but not in VGAT-Cre$^{hrGFP/VMP}$ mice. RN, red nucleus; VTA, ventral tegmental area; SN, substantia nigra; IP, interpeduncular nucleus. Scale bar, 500 μm.

Figure 1. *Continued*

(C) Representative path traces and total distance traveled in the open field test. Two-tailed unpaired *t* test, $t = 4.418$, $df = 17$, $p = 0.0004$.

(D) Immobility time in the tail suspension test. Two-tailed unpaired *t* test, $t = 3.238$ $df = 17$, $p = 0.0048$.

(E) Immobility time in the forced swim test. Two-tailed Mann-Whitney *U* test, $U = 0$, $p < 0.0001$.

(F) Sociability and social interaction test. Preference for the zone with mouse chamber compared with the empty chamber. Two-tailed unpaired *t* test, $t = 2.319$, $df = 17$, $p = 0.0331$.

(G) Time in open arms in the elevated plus maze. Two-tailed unpaired *t* test, $t = 3.214$, $df = 16$, $p = 0.0054$.

(H) Nest-building scores. Two-tailed unpaired *t* test, $t = 4.52$, $df = 17$, $p = 0.0003$.

(I) Exploratory preference toward familiar or novel objects in the novel object recognition task on the test day. VGAT-Cre$^{hrGFP/VMP}$: two-tailed unpaired *t* test, $t = 4.742$, $df = 18$, $p = 0.0002$. VGAT-Cre$^{DTA/VMP}$: two-tailed unpaired *t* test, $t = 1.592$, $df = 16$, $p = 0.1308$.

(J) Total number of entries into each arm and spontaneous alternation rates in the Y-maze task. Number of arm entries: two-tailed unpaired *t* test, $t = 3.159$, $df = 17$, $p = 0.0057$. Spontaneous alternation rate: two-tailed unpaired *t* test, $t = 1.165$, $df = 17$, $p = 0.2601$.

(C–J) $n = 8$–10 mice for each group. Individual values are plotted in the graphs. Data are presented as the mean ± SEM. n.s., not significant, $*p < 0.05$, $**p < 0.01$, $***p < 0.001$, $****p < 0.0001$.

with mice compared with control VGAT-Cre$^{hrGFP/VMP}$ mice ($p < 0.05$, Figure 1F). In the elevated plus maze, VGAT-Cre$^{DTA/VMP}$ mice spent more time in the open arms ($p < 0.01$, Figure 1G), indicating less anxiety and increased risk-taking behavior. In addition, VGAT-Cre$^{DTA/VMP}$ mice had lower scores in the nest building test ($p < 0.001$, Figure 1H). We also assessed learning and memory. In the novel object recognition task, control VGAT-Cre$^{hrGFP/VMP}$ mice showed increased exploratory preference for novel objects ($p < 0.001$, Figure 1I). On the other hand, VGAT-Cre$^{DTA/VMP}$ mice demonstrated no preference for novel objects (not significant, n.s., $p = 0.131$, Figure 1I), suggesting impaired novel object recognition. Conversely, in the Y maze as a test for working memory, VGAT-Cre$^{DTA/VMP}$ mice exhibited no difference from control mice in spontaneous alternation rate (n.s., $p = 0.260$, Figure 1J), but the number of entries into each arm was increased, consistent with their hyperactivity ($p < 0.01$, Figure 1J). Overall, the series of behavioral tests provided us landmark information to support the involvement of VMP GABAergic neurons in the various aspects of manic episodes described in both humans and rodent models (American Psychiatric Association, 2013; Logan and McClung, 2016; Perry et al., 2009; Young et al., 2007), including hyperactivity, reduced depression and anxiety, and risk-taking behavior. Together with these core components, one of the prominent symptoms of mania is a decreased need for sleep (American Psychiatric Association, 2013; World Health Organization, 2004), which helps to discriminate mania from other disorders with hyperactivity, e.g., attention-deficit/hyperactivity disorder (Marangoni et al., 2015). Therefore, we next performed a detailed analysis of the sleep/wake behaviors in VGAT-Cre$^{DTA/VMP}$ mice.

GABAergic VMP Ablation Induces Reduced Daily Sleep Amounts and Loss of Rebound Sleep

Sleep consists of rapid eye movement sleep (REMS) and slow-wave sleep (SWS), also known as non-REM sleep, which are distinguished on the basis of electroencephalography (EEG) and electromyography (EMG) characteristics. It is commonly considered that sleep need is represented during SWS as EEG power in delta frequency (0.5–4 Hz), which increases in animals after prolonged wakefulness (Daan et al., 1984; Lazarus et al., 2019) as well as in mutant mice with prolonged daily sleep amount (Funato et al., 2016; Honda et al., 2018). We first measured the daily sleep amount of VGAT-Cre$^{DTA/VMP}$ mice. The VGAT-Cre$^{DTA/VMP}$ mice displayed reduced sleep amounts and increased wake amounts compared with control VGAT-Cre$^{hrGFP/VMP}$ mice (SWS 24 h: $p < 0.0001$, SWS light: $p < 0.0001$, SWS dark: $p < 0.001$, wake 24 h: $p < 0.0001$, wake light: $p < 0.0001$, wake dark: $p < 0.001$, REMS 24 h: $p < 0.001$, REMS light: $p < 0.0001$, REMS dark: $p < 0.05$, Figures 2A and 2B), consistent with our previous study (Takata et al., 2018). Next, we calculated the delta power during daily SWS to evaluate the mean level of sleep need. In contrast to the severe sleep reduction in VGAT-Cre$^{DTA/VMP}$ mice, there was no difference in the EEG power spectra ($p = 0.650$, Figure S1) and the delta power ($p = 0.378$, Figure 2C) during SWS over 24 h compared with control VGAT-Cre$^{hrGFP/VMP}$ mice. This finding suggests that VGAT-Cre$^{DTA/VMP}$ mice are able to maintain the same level of sleep need compared with control mice, despite lower daily sleep amounts. Alternatively, although the daily sleep amount is constantly reduced, it would be an adequate amount for VGAT-Cre$^{DTA/VMP}$ mice such that it does not evoke changes in the mean level of the SWS delta power. Thus, VGAT-Cre$^{DTA/VMP}$ mice may not be under higher sleep pressure or suffering from greater "sleepiness" despite the reduced sleep amounts. To further investigate sleep/wake phenotypes, we performed sleep deprivation (SD) experiments.

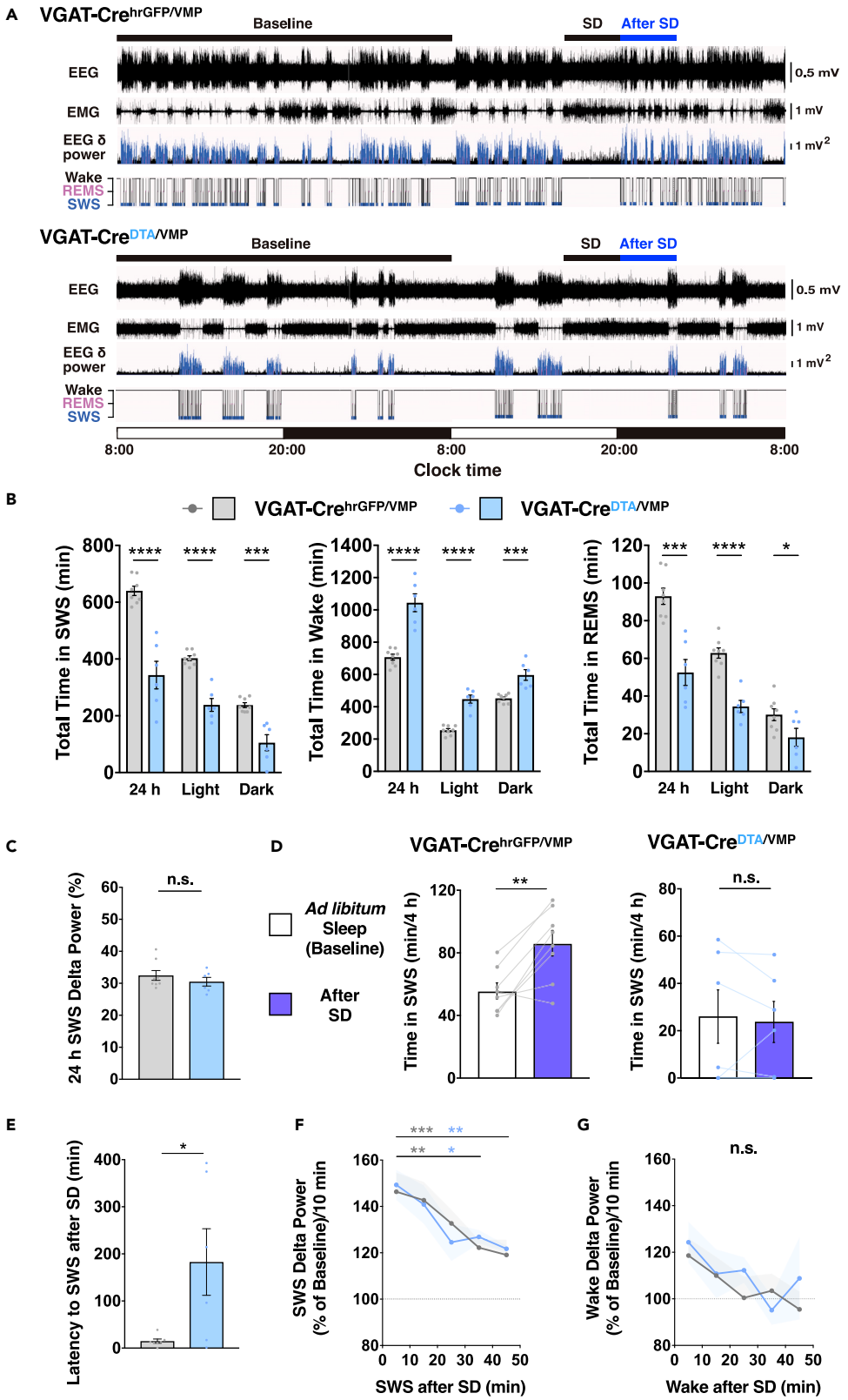
A
VGAT-CrehrGFP/VMP
Baseline
SD
After SD
EEG
EMG
EEG δ power
Wake
REMS
SWS
0.5 mV
1 mV
1 mV2
VGAT-CreDTA/VMP
8:00
20:00
8:00
20:00
8:00
Clock time
B
VGAT-CrehrGFP/VMP
VGAT-CreDTA/VMP
Total Time in SWS (min)
Total Time in Wake (min)
Total Time in REMS (min)
24 h
Light
Dark
C
24 h SWS Delta Power (%)
n.s.
D
Ad libitum Sleep (Baseline)
After SD
Time in SWS (min/4 h)
E
Latency to SWS after SD (min)
F
SWS Delta Power (% of Baseline)/10 min
SWS after SD (min)
G
Wake Delta Power (% of Baseline)/10 min
Wake after SD (min)

Figure 2. Selective Ablation of the VMP GABAergic Neurons Induces Reduced Daily Sleep Amounts and Loss of Sleep Rebound

(A) EEG, EMG, EEG delta power, and wake/REMS/SWS hypnogram. SD, sleep deprivation.

(B) Total time in SWS, wake, and REMS during 24 h, light and dark periods on the baseline day. SWS 24 h: two-tailed unpaired *t* test, $t = 6.484$, $df = 12$, $p < 0.0001$. SWS light: two-tailed unpaired *t* test, $t = 7.579$, $df = 12$, $p < 0.0001$. SWS dark: two-tailed unpaired *t* test, $t = 5.06$, $df = 12$, $p = 0.0003$. Wake 24 h: two-tailed unpaired *t* test, $t = 6.503$, $df = 12$, $p < 0.0001$. Wake light: two-tailed unpaired *t* test, $t = 7.855$, $df = 12$, $p < 0.0001$. Wake dark: two-tailed unpaired *t* test, $t = 4.756$, $df = 12$, $p = 0.0005$. REMS 24 h: two-tailed unpaired *t* test, $t = 5.231$, $df = 12$, $p = 0.0002$. REMS light: two-tailed unpaired *t* test, $t = 6.736$, $df = 12$, $p < 0.0001$. REMS dark: two-tailed unpaired *t* test, $t = 2.2$, $df = 12$, $p = 0.0481$.

(C) Average of delta power (%) during SWS across 24 h on the baseline day. Two-tailed unpaired *t* test, $t = 0.9161$, $df = 12$, $p = 0.3777$.

(D) Sleep rebound. Time in SWS during 4 h (20:00–24:00) *ad libitum* sleep (baseline) and after SD. VGAT-Cre$^{hrGFP/VMP}$: two-tailed paired *t* test, $t = 4.266$, $df = 7$, $p = 0.0037$. VGAT-Cre$^{DTA/VMP}$: two-tailed paired *t* test, $t = 0.4298$, $df = 5$, $p = 0.6852$.

(E) Latency to first SWS episode after SD. Two-tailed unpaired *t* test, $t = 2.579$, $df = 11$, $p = 0.0256$.

(F) Time course of delta power change during SWS after SD compared with baseline delta power. Baseline delta power is the averaged absolute value of delta power during SWS across 24 h on the baseline day. Two-way repeated measures ANOVA followed by Sidak's multiple comparisons. $F(1, 11) = 0.00004835$, $p = 0.9946$, the main effect of viral transduction. $F(4, 44) = 12.87$, $p < 0.0001$, the main effect of time. VGAT-Cre$^{hrGFP/VMP}$: 0–10 min versus 30–40 min, $p = 0.0012$; 0–10 min versus 40–50 min, $p = 0.0002$. VGAT-Cre$^{DTA/VMP}$: 0–10 min versus 30–40 min, $p = 0.0323$; 0–10 min versus 40–50 min, $p = 0.0041$.

(G) Time course of delta power change during wake after SD compared with baseline delta power. Baseline delta power is the averaged absolute value of delta power during wake across 24 h on the baseline day. Two-way repeated measures ANOVA. $F(1, 9) = 0.3214$, $p = 0.5846$, the main effect of viral transduction. $F(4, 36) = 2.341$, $p = 0.0735$, the main effect of time.

(B–G) $n = 5$–8 mice for each group. Individual values are plotted in the graphs. Data are presented as the mean ± SEM. n.s., not significant, *$p < 0.05$, **$p < 0.01$, ***$p < 0.001$, ****$p < 0.0001$. See also Figure S1.

Prolonged wakefulness with SD leads to an increase in the sleep period by so-called sleep homeostasis (Campbell and Tobler, 1984; Hendricks et al., 2000) among animals. In this study, a normal sleep rebound after SD was observed in control VGAT-Cre$^{hrGFP/VMP}$ mice ($p < 0.01$, Figure 2D), whereas VGAT-Cre$^{DTA/VMP}$ mice did not exhibit sleep rebound after 4-h SD (n.s., $p = 0.685$, Figure 2D), suggesting less sleep pressure after SD in VGAT-Cre$^{DTA/VMP}$ mice.

Although the sleep latency after SD was extended in VGAT-Cre$^{DTA/VMP}$ mice ($p < 0.05$, Figure 2E), we found that EEG delta power during SWS was increased after SD and dissipated along with SWS time (not total time) in VGAT-Cre$^{DTA/VMP}$ mice (0–10 min versus 30–40 min: $p < 0.05$, 0–10 min versus 40–50 min: $p < 0.01$, Figure 2F), despite lacking sleep rebound (Figure 2D). These data suggest that the mechanisms regulating delta power during SWS and sleep amounts are dissociable, consistent with findings from a previous study (Suzuki et al., 2013). Remarkably, SWS delta power dissipation along with SWS time after SD was noticeably similar between VGAT-Cre$^{DTA/VMP}$ and the control VGAT-Cre$^{hrGFP/VMP}$ mice (n.s., $p = 0.995$, the main effect of viral transduction, ANOVA; Figure 2F). In contrast, the gradual decay of delta power was not observed during wakefulness (n.s., $p = 0.074$, the main effect of time, ANOVA; Figure 2G). These observations suggest that the neural mechanisms generate delta power after SD function mainly during SWS and pause during wakefulness. Overall, we revealed that VMP GABAergic neurons have critical roles in the regulation of both daily sleep amounts and homeostatic sleep as a response to SD.

Dopamine D_2 Receptors Mediate Sleep Reduction Induced by GABAergic VMP Ablation

Our previous pharmacologic study suggested that D_2 and/or D_3 receptors mediate the wake-promoting effect induced by ablating or inhibiting VMP GABAergic neurons (Takata et al., 2018). To evaluate the involvement of D_2 receptors (D_2R) in notable behaviors in VGAT-Cre$^{DTA/VMP}$ mice, we generated D_2R knockout (KO) mice using fertilized egg donors of VGAT-Cre mice by the CRISPR-Cas9 technique (VGAT-Cre;$D_2R^{-/-}$ mice; Figure 3A). We first histologically confirmed that immunostaining for D_2R was only detected in VGAT-Cre;$D_2R^{+/+}$ mice and not in VGAT-Cre;$D_2R^{-/-}$ mice (Figure 3B). To verify an *in vivo* functional D_2R deficit, we administered a moderate dose (45 mg/kg) of modafinil, a dopamine transporter blocker that has an arousal effect and is largely ineffective in D_2R-deficient mice (Qu et al., 2008). Consistent with the previous study, our newly generated VGAT-Cre;$D_2R^{-/-}$ mice did not exhibit arousal after modafinil administration ($p = 0.788$, Figure 3C), in contrast to the significant arousal effect observed in VGAT-Cre;$D_2R^{+/+}$ mice ($p < 0.001$, Figure 3C).

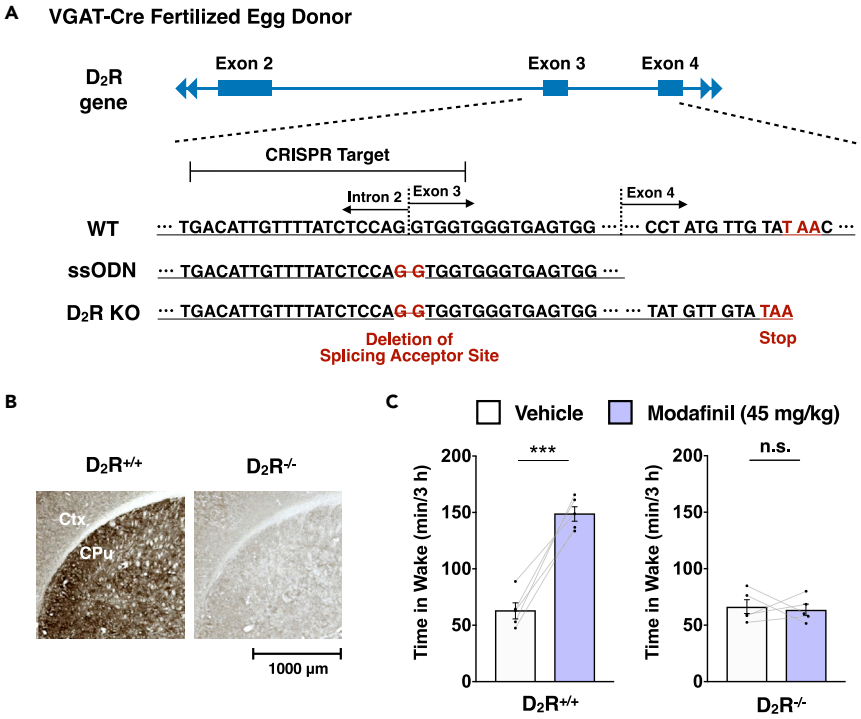

Figure 3. Generation of D_2R Knockout VGAT-Cre Mice by the CRISPR/Cas9 System

(A) Schematic of CRISPR/Cas9-mediated D_2R gene knockout using the fertilized egg donor of VGAT-Cre mice. The CRISPR target including the PAM sequence (total 23 bp) contains the part of intron 2 and exon 3 of the D_2R gene encompassing the splicing acceptor (SA) site. ssODN, single-stranded oligodeoxynucleotide.

(B) Histologic verification of D_2R knockout. Immunostained D_2R signals were only detected in $D_2R^{+/+}$ mice and not in $D_2R^{-/-}$ mice. Ctx, cortex; CPu, caudate putamen (striatum). Scale bar represents 1,000 μm.

(C) *In vivo* functional verification of D_2R knockout based on the loss of modafinil-induced arousal in $D_2R^{-/-}$ mice. $D_2R^{+/+}$: two-tailed paired *t* test, $t = 9.164$, $df = 4$, $p = 0.0008$. $D_2R^{-/-}$: two-tailed paired *t* test, $t = 0.2872$, $df = 4$, $p = 0.7882$. $n = 5$ mice for each group. Individual values are plotted in the graphs.

Data are presented as the mean ± SEM. n.s., not significant, ***$p < 0.001$.

To assess the D_2R involvement in sleep behaviors in VGAT-$Cre^{DTA/VMP}$ mice, we next injected AAV-FLEX-DTA or control AAV-FLEX-hrGFP virus into the VMP of VGAT-Cre;$D_2R^{+/+}$ mice or VGAT-Cre;$D_2R^{-/-}$ mice. We first confirmed that VGAT-$Cre^{DTA/VMP}$;$D_2R^{+/+}$ mice exhibited reduced amounts of SWS over 24 h ($p < 0.0001$, the main effect of viral transduction, ANOVA; Figure 4A) in both light and dark periods (light: $p < 0.001$, dark: $p < 0.01$, Figure 4B) compared with control VGAT-$Cre^{hrGFP/VMP}$;$D_2R^{+/+}$ mice. Although VGAT-$Cre^{DTA/VMP}$;$D_2R^{-/-}$ mice also showed reduced SWS amounts over 24 h ($p < 0.001$, the main effect of viral transduction, ANOVA; Figure 4C), strikingly, VGAT-$Cre^{DTA/VMP}$;$D_2R^{-/-}$ mice showed no difference in SWS amounts during the light period compared with control VGAT-$Cre^{hrGFP/VMP}$;$D_2R^{-/-}$ mice (light: n.s., $p = 0.182$, dark: $p < 0.001$, Figure 4D). In other words, the reduced sleep amounts observed in VGAT-$Cre^{DTA/VMP}$ mice during the light period (Figure 2B) were functionally rescued by the loss of D_2R. This finding indicates that the sleep reduction induced by ablating VMP GABAergic neurons is mainly mediated by D_2R.

We next examined the effect of SD, which resulted in the loss of rebound sleep by ablation of VMP GABAergic neurons regardless of $D_2R^{+/+}$ or $D_2R^{-/-}$ conditions ($p = 0.111$, VGAT-$Cre^{DTA/VMP}$;$D_2R^{+/+}$ basal versus SD; $p = 0.406$, VGAT-$Cre^{DTA/VMP}$;$D_2R^{-/-}$ basal versus SD; Figure 4E), suggesting that the impaired sleep homeostasis in VGAT-$Cre^{DTA/VMP}$ mice (Figure 2D) is D_2R independent. Similarly, the extended latency to SWS after SD (Figure 2E) was D_2R-independent ($p < 0.05$, VGAT-$Cre^{hrGFP/VMP}$;$D_2R^{+/+}$ versus VGAT-$Cre^{DTA/VMP}$;$D_2R^{+/+}$; $p < 0.05$, VGAT-$Cre^{hrGFP/VMP}$;$D_2R^{-/-}$ versus VGAT-$Cre^{DTA/VMP}$;$D_2R^{-/-}$; Figure 4F).

We then assessed VGAT-$Cre^{DTA/VMP}$ mice in a set of behavioral tasks to examine the D_2R dependency of hyperactivity and anti-depressive behaviors. In the open field test, both VGAT-$Cre^{DTA/VMP}$;$D_2R^{+/+}$ and VGAT-$Cre^{DTA/VMP}$;$D_2R^{-/-}$ mice exhibited increased travel distance ($p < 0.01$, VGAT-$Cre^{hrGFP/VMP}$;$D_2R^{+/+}$ versus

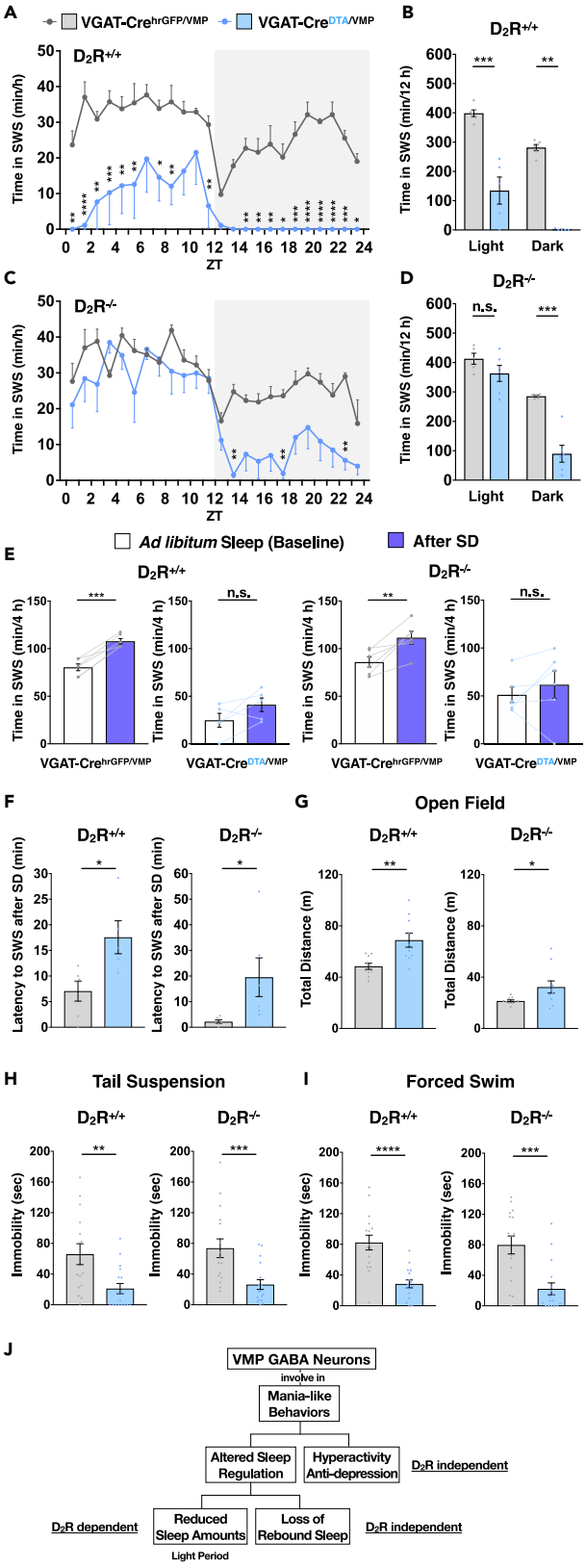
A
VGAT-CrehrGFP/VMP
VGAT-CreDTA/VMP
D2R+/+
Time in SWS (min/h)
ZT
B
D2R+/+
Time in SWS (min/12 h)
Light
Dark
C
D2R-/-
D
D2R-/-
n.s.
E
Ad libitum Sleep (Baseline)
After SD
D2R+/+
D2R-/-
Time in SWS (min/4 h)
F
Latency to SWS after SD (min)
G
Open Field
Total Distance (m)
H
Tail Suspension
Immobility (sec)
I
Forced Swim
J
VMP GABA Neurons
involve in
Mania-like Behaviors
Altered Sleep Regulation
Hyperactivity Anti-depression
D2R independent
D2R dependent
Reduced Sleep Amounts
Light Period
Loss of Rebound Sleep
D2R independent

Figure 4. Dopamine D_2R Mediate Sleep Reduction Induced by GABAergic VMP Ablation

(A) Hourly SWS amounts in $D_2R^{+/+}$ mice. Two-way repeated measures ANOVA followed by Sidak's multiple comparisons. F (1, 9) = 139.5, $p < 0.0001$, the main effect of viral transduction.

(B) Total SWS amounts in $D_2R^{+/+}$ mice. Light: two-tailed unpaired t test, $t = 6.057$, $df = 9$, $p = 0.0002$. Dark: two-tailed Mann-Whitney U test, $U = 0$, $p = 0.0043$.

(C) Hourly SWS amounts in $D_2R^{-/-}$ mice. Two-way repeated measures ANOVA followed by Sidak's multiple comparisons. F (1, 9) = 24.86, $p = 0.0008$, the main effect of viral transduction.

(D) Total SWS amounts in $D_2R^{-/-}$ mice. Light: two-tailed unpaired t test, $t = 1.447$, $df = 9$, $p = 0.1817$. Dark: two-tailed unpaired t test, $t = 6.14$, $df = 9$, $p = 0.0002$.

(E) Sleep rebound. Time in SWS during 4 h (20:00–24:00) *ad libitum* sleep (baseline) and after SD. VGAT-$Cre^{hrGFP/VMP}$;$D_2R^{+/+}$: two-tailed paired t test, $t = 8.863$, $df = 5$, $p = 0.0003$. VGAT-$Cre^{DTA/VMP}$;$D_2R^{+/+}$: two-tailed paired t test, $t = 2.042$, $df = 4$, $p = 0.1107$. VGAT-$Cre^{hrGFP/VMP}$;$D_2R^{-/-}$: two-tailed paired t test, $t = 4.091$, $df = 5$, $p = 0.0094$. VGAT-$Cre^{DTA/VMP}$;$D_2R^{-/-}$: two-tailed paired t test, $t = 0.9074$, $df = 5$, $p = 0.4058$.

(F) Latency to first SWS episode after SD. $D_2R^{+/+}$: two-tailed unpaired t test, $t = 2.902$, $df = 9$, $p = 0.0175$. $D_2R^{-/-}$: two-tailed unpaired t test, $t = 2.287$, $df = 10$, $p = 0.0452$.

(G) Total distance traveled in the open field test. $D_2R^{+/+}$: two-tailed unpaired t test, $t = 3.411$, $df = 18$, $p = 0.0031$. $D_2R^{-/-}$: two-tailed unpaired t test, $t = 2.261$, $df = 18$, $p = 0.0364$.

(H) Immobility time in the tail suspension test. $D_2R^{+/+}$: two-tailed unpaired t test, $t = 3.064$, $df = 30$, $p = 0.0046$. $D_2R^{-/-}$: two-tailed Mann-Whitney U test, $U = 45.5$, $p = 0.0007$.

(I) Immobility time in the forced swim test. $D_2R^{+/+}$: two-tailed unpaired t test, $t = 4.952$, $df = 30$, $p < 0.0001$. $D_2R^{-/-}$: two-tailed Mann-Whitney U test, $U = 42.5$, $p = 0.0004$.

(J) Schematic model. VMP GABAergic neurons involved in the genesis of mania-like behaviors, including hyperactivity, anti-depressive behaviors, and reduced sleep. The reduced sleep amounts due to dysfunction of VMP GABAergic neurons were mediated in a D_2R-dependent manner.

(A–I) n = 5–17 mice for each group. Individual values are plotted in the graphs. Data are presented as the mean ± SEM. n.s., not significant, *$p < 0.05$, **$p < 0.01$, ***$p < 0.001$, ****$p < 0.0001$.

VGAT-$Cre^{DTA/VMP}$;$D_2R^{+/+}$; $p < 0.05$, VGAT-$Cre^{hrGFP/VMP}$;$D_2R^{-/-}$ versus VGAT-$Cre^{DTA/VMP}$;$D_2R^{-/-}$; Figure 4G) demonstrating that the hyperactivity in VGAT-$Cre^{DTA/VMP}$ mice (Figure 1C) is D_2R independent. Consistently, a decreased immobility in both the tail suspension test and forced swim test was observed regardless of $D_2R^{+/+}$ or $D_2R^{-/-}$ conditions (tail suspension: $p < 0.01$, VGAT-$Cre^{hrGFP/VMP}$;$D_2R^{+/+}$ versus VGAT-$Cre^{DTA/VMP}$;$D_2R^{+/+}$; $p < 0.001$, VGAT-$Cre^{hrGFP/VMP}$;$D_2R^{-/-}$ versus VGAT-$Cre^{DTA/VMP}$;$D_2R^{-/-}$; Figure 4H; and forced swim: $p < 0.0001$, VGAT-$Cre^{hrGFP/VMP}$;$D_2R^{+/+}$ versus VGAT-$Cre^{DTA/VMP}$;$D_2R^{+/+}$; $p < 0.001$, VGAT-$Cre^{hrGFP/VMP}$;$D_2R^{-/-}$ versus VGAT-$Cre^{DTA/VMP}$;$D_2R^{-/-}$, Figure 4I), suggesting that the phenotypes consistent with anti-depressive behaviors in VGAT-$Cre^{DTA/VMP}$ mice (Figures 1D and 1E) are also D_2R independent.

DISCUSSION

In the present study, we found that ablating GABAergic neurons in the VMP induced various behavioral phenotypes, including hyperactivity, reduced depression and anxiety, loss of sleep rebound, and reduced sleep. The phenotypes in VGAT-$Cre^{DTA/VMP}$ mice with hyperactivity in the open field (Figure 1C), reduced immobility in tail suspension (Figure 1D) and forced swim tests (Figure 1E), and increased social interaction (Figure 1F) may be consistent with the facets of mania symptoms in humans, such as increased goal-directed activity and psychomotor agitation, which is described in the Diagnostic and Statistical Manual of Mental Disorders (DSM-5) (American Psychiatric Association, 2013; Johnson, 2005). Hyperactivity and reduced depression are common features in the reported genetic mouse models of mania, including *Shank3*-overexpression (Han et al., 2013) and *GSK3-β*-overexpression mutants (Prickaerts et al., 2006). Importantly, objectively measured high locomotor activity in manic patients quantitively bears a resemblance to the hyperactivity in hyperdopaminergic rodent models on the basis of cross-species translational studies (Perry et al., 2009; Young et al., 2007, 2011a). Further, activation of dopaminergic neurons in the ventral tegmental area (VTA) induces hyperactivity in rodents (Boekhoudt et al., 2016). Because the VTA region is anatomically included in the VMP (Figure 1B), ablation of VMP GABAergic neurons may unlock inhibitory outputs on VTA dopaminergic neurons, which could lead to locomotor hyperactivity. To further dissect the detailed mechanisms underlying hyperactivity phenotypes in future studies, dopamine levels should be measured around the nucleus accumbens, a major target area of the VTA, in VGAT-$Cre^{DTA/VMP}$ mice. The reduced anxiety and increased risk-taking behavior of VGAT-$Cre^{DTA/VMP}$ mice in the elevated plus maze (Figure 1G) are presumably related to excessive involvement in activities with a high potential for a painful consequence in humans (American Psychiatric Association, 2013; Leahy, 1999). Increased risk-taking behaviors are also reported in both manic patients and dopamine transporter knockdown (DAT-KD) hyperdopaminergic mice using comparable tasks (van Enkhuizen et al., 2014; Young et al., 2011b). In addition, the low nest-building performance (Figure 1H) supports the aspect of distractibility described in the

diagnostic criteria (American Psychiatric Association, 2013; Oltmanns, 1978; World Health Organization, 2004). VGAT-Cre$^{DTA/VMP}$ mice exhibited impaired novel object recognition (Figure 1I), whereas alternation rate in the Y-maze was intact, suggesting that VGAT-Cre$^{DTA/VMP}$ mice could remember and refer to the location of the arm they entered previously as working memory during the task. In contrast to the Y maze task, the novel object recognition task has a 24-h test interval (see Transparent Methods), allowing mice to have sleep states and suggesting the possible contribution of sleep to memory consolidation in this specific task. Sleep deprivation or disruption impairs the performance of novel object recognition in mice (Palchykova et al., 2006; Rolls et al., 2011). Thus, the reduced sleep in VGAT-Cre$^{DTA/VMP}$ mice may account for their impaired performance in the novel object recognition task. The largely abolished daily sleep amounts in VGAT-Cre$^{DTA/VMP}$ mice (Figures 2A and 2B) are consistent with decreased need for sleep in manic individuals (American Psychiatric Association, 2013; World Health Organization, 2004) and *Clock*Δ*19* mutant mice (Naylor et al., 2000), a well-characterized genetic model of mania (Logan and McClung, 2016).

Although some genes, cells, or neural circuits in mammals are suggested to have roles in homeostatic sleep regulation (Halassa et al., 2009; Hayaishi et al., 2004; Ma et al., 2019), the detailed mechanisms remain largely unknown. On the other hand, some behaviors can overcome the homeostatic sleep pressure, even after long-lasting wakefulness. For example, SD induced by an environmental change such as cage exchange shows markedly less sleep rebound compared with gentle handling in mice (Suzuki et al., 2013). VGAT-Cre$^{DTA/VMP}$ mice did not show sleep rebound after SD (Figure 2D), indicating that either the VMP GABAergic neurons are critical for producing sleep states in response to SD or the behaviors induced by the loss of the neurons overcame the homeostatic sleep pressure induced by SD.

Increasing evidence indicates that dopamine and D_2R promote wakefulness to suppress sleep (Oishi and Lazarus, 2017; Oishi et al., 2017; Qu et al., 2008, 2010). In this study, using a constitutive genetic D_2R KO (Figure 3), we clarified that sleep loss (promoting wake) in VGAT-Cre$^{DTA/VMP}$ mice was dependent on D_2R, at least during the light period (Figure 4). These data imply that the VMP GABAergic neurons suppress mainly dopaminergic systems and D_2R to presumably prevent excessive amounts of wakefulness. It is unclear which dopaminergic systems are suppressed by the VMP. Anatomic studies (Jhou et al., 2009a, 2009b; Omelchenko and Sesack, 2009; Taylor et al., 2014) indicate that the GABAergic VTA and rostromedial tegmental nucleus, both of which are included in the VMP, innervate dopaminergic neurons in the VTA and dorsal raphe nucleus (DRN), also known as the ventral periaqueductal gray matter, which regulate wakefulness (Cho et al., 2017; Eban-Rothschild et al., 2016; Lu et al., 2006; Oishi et al., 2017; Taylor et al., 2016). The functional relationship between VMP and these dopaminergic areas should be examined in the future. Serotonin (5-HT) is also involved in regulating both sleep/wake and locomotor activity (Correia et al., 2017; Saper et al., 2005). Studies in both humans and mice suggest that serotonin is involved in mania and its treatment (Maddaloni et al., 2018; Shiah and Yatham, 2000). In this sense, investigating the loss of VMP GABAergic innervation to DRN serotonergic neurons is another potential study direction.

The mechanisms related to hyperactivity, anti-depressive behaviors, and reduced sleep amount during the dark period in VGAT-Cre$^{DTA/VMP}$ mice remain unclear. Recent studies revealed GABAergic projections from the VTA to the lateral hypothalamus (Taylor et al., 2014; Yu et al., 2019) and especially onto orexin neurons (Chowdhury et al., 2019), which are critical for maintaining wakefulness (Chemelli et al., 1999). Optogenetic activation of GABAergic VTA terminals in the lateral hypothalamus suppresses wakefulness (Chowdhury et al., 2019; Yu et al., 2019). Moreover, lateral hypothalamic kindling induces mania-like behaviors (Abulseoud et al., 2014). Therefore, the lateral hypothalamus might play a role in the mania-like behaviors induced by GABAergic VMP ablation.

In summary, as illustrated in Figure 4J, our findings revealed that VMP GABAergic neurons are involved in various aspects of mania-like behaviors, and the reduced sleep amounts are mediated through the D_2R-dependent dopaminergic system. Further research using VGAT-Cre$^{DTA/VMP}$ mice may help to elucidate the different aspects of mania as well as the detailed neural mechanisms of sleep homeostasis and contribute to the development of safer and more effective drugs.

Limitations of the Study

Pharmacological studies in VGAT-Cre$^{DTA/VMP}$ mice, such as of lithium and valproic acid, which are the commonly used treatments for bipolar disorder (Chiu et al., 2013; Logan and McClung, 2016), are important for further investigation of the effects on individual behavioral phenotypes and D_2R-dependency. Because all the experiments were performed using male mice in the present study, investigating the phenotypical difference with female mice provides further information about our findings.

Resource Availability

Lead Contact

Further information and requests for reagents and resources should be directed to and will be fulfilled by the Lead Contact, Yo Oishi (oishi.yo.fu@u.tsukuba.ac.jp).

Materials Availability

The mouse line generated in this study (D_2R KO strain) will be made available with a completed Material Transfer Agreement.

Data and Code Availability

The data that support the findings of this study are available from the Lead Contact on reasonable request.

METHODS

All methods can be found in the accompanying Transparent Methods supplemental file.

SUPPLEMENTAL INFORMATION

Supplemental Information can be found online at https://doi.org/10.1016/j.isci.2020.101240.

ACKNOWLEDGMENTS

We thank WPI-IIIS Lazarus/Oishi laboratory and Yanagisawa/Funato laboratory members for suggestions and comments. We also thank M. Sakaguchi, Y. Hayashi, S. Takenawa and K. Kobayashi for their technical advice and support. This work was supported by the Japan Society for the Promotion of Science (JSPS) KAKENHI Grants 15J06369 (to T.H.), 19K06950 (to Y.T.), 17H02215 (to M.L.) and 18H02534 (to Y.O.); JSPS Overseas Research Fellowship (to T.H.); Takeda Science Foundation (to Y.O.); JST-Mirai Program JPMJMI19D8 (to Y.O.); the Japan Foundation for Applied Enzymology (to Y.O.); the Japan Science and Technology Agency CREST Grant JPMJCR1655 (to M.L. and M.Y.); the Ministry of Education, Culture, Sports, Science and Technology (MEXT) of Japan Grants-in-Aid for Scientific Research on Innovative Areas "WillDynamics" 19H05004 (to M.L.); the World Premier International Research Center Initiative (WPI) from MEXT (to T.H., Y.T., Y.C., S.T., H.F., M.Y., M.L., and Y.O.).

AUTHOR CONTRIBUTIONS

Conceptualization, T.H. and Y.O.; Investigation, T.H., Y.T., and Y.O.; Resources, Y.C., S.M., F.S., and S.T.; Writing—Original Draft, T.H. and Y.O.; Writing—Review & Editing, Y.T., Y.C., S.M., F.S., S.T., H.F., M.Y., and M.L.; Supervision, T.H., M.L., and Y.O.

DECLARATION OF INTERESTS

The authors declare no competing interests.

Received: February 10, 2020
Revised: May 4, 2020
Accepted: June 2, 2020
Published: June 26, 2020

REFERENCES

Abulseoud, O.A., Camsari, U.M., Ruby, C.L., Mohamed, K., Abdel Gawad, N.M., Kasasbeh, A., Yuksel, M.Y., and Choi, D.S. (2014). Lateral hypothalamic kindling induces manic-like behavior in rats: a novel animal model. Int. J. Bipol. Disord. *2*, 7.

American Psychiatric Association. (2013). Diagnostic and Statistical Manual of Mental Disorders, 5th Edition: DSM-5 (American Psychiatric Publishing).

Antelmi, E., Fabbri, M., Cretella, L., Guarino, M., and Stracciari, A. (2014). Late onset bipolar disorder due to a lacunar state. Behav. Neurol. *2014*, 780742.

Benca, R.M., Okawa, M., Uchiyama, M., Ozaki, S., Nakajima, T., Shibui, K., and Obermeyer, W.H. (1997). Sleep and mood disorders. Sleep Med. Rev. *1*, 45–56.

Boekhoudt, L., Omrani, A., Luijendijk, M.C.M., Wolterink-Donselaar, I.G., Wijbrans, E.C., van der Plasse, G., and Adan, R.A.H. (2016). Chemogenetic activation of dopamine neurons in the ventral tegmental area, but not substantia nigra, induces hyperactivity in rats. Eur. Neuropsychopharmacol. *26*, 1784–1793.

Campbell, S.S., and Tobler, I. (1984). Animal sleep: a review of sleep duration across phylogeny. Neurosci. Biobehav. Rev. *8*, 269–300.

Caplan, L.R. (2010). Delirium: a neurologist's view–the neurology of agitation and overactivity. Rev. Neurol. Dis. *7*, 111–118.

Chemelli, R.M., Willie, J.T., Sinton, C.M., Elmquist, J.K., Scammell, T., Lee, C., Richardson,

J.A., Williams, S.C., Xiong, Y., Kisanuki, Y., et al. (1999). Narcolepsy in orexin knockout mice: molecular genetics of sleep regulation. Cell *98*, 437–451.

Chiu, C.-T., Wang, Z., Hunsberger, J.G., and Chuang, D.-M. (2013). Therapeutic potential of mood stabilizers lithium and valproic acid: beyond bipolar disorder. Pharmacol. Rev. *65*, 105–142.

Cho, J.R., Treweek, J.B., Robinson, J.E., Xiao, C., Bremner, L.R., Greenbaum, A., and Gradinaru, V. (2017). Dorsal raphe dopamine neurons modulate arousal and promote wakefulness by salient stimuli. Neuron *94*, 1205–1219.e8.

Chowdhury, S., Matsubara, T., Miyazaki, T., Ono, D., Fukatsu, N., Abe, M., Sakimura, K., Sudo, Y., and Yamanaka, A. (2019). GABA neurons in the ventral tegmental area regulate non-rapid eye movement sleep in mice. Elife *8*, e44928.

Correia, P.A., Lottem, E., Banerjee, D., Machado, A.S., Carey, M.R., and Mainen, Z.F. (2017). Transient inhibition and long-term facilitation of locomotion by phasic optogenetic activation of serotonin neurons. Elife *6*, e20975.

Crawley, J.N. (2007). What's Wrong with My Mouse? Behavioral Phenotyping of Transgenic and Knockout Mice, Second Edition (John Wiley & Sons Inc).

Crawley, J.N., and Paylor, R. (1997). A proposed test battery and constellations of specific behavioral paradigms to investigate the behavioral phenotypes of transgenic and knockout mice. Horm. Behav. *31*, 197–211.

Daan, S., Beersma, D.G., and Borbely, A.A. (1984). Timing of human sleep: recovery process gated by a circadian pacemaker. Am. J. Physiol. *246*, R161–R183.

Drake, M.E., Jr., Pakalnis, A., and Phillips, B. (1990). Secondary mania after ventral pontine infarction. J. Neuropsychiatry Clin. Neurosci. *2*, 322–325.

Eban-Rothschild, A., Rothschild, G., Giardino, W.J., Jones, J.R., and de Lecea, L. (2016). VTA dopaminergic neurons regulate ethologically relevant sleep-wake behaviors. Nat. Neurosci. *19*, 1356–1366.

Funato, H., Miyoshi, C., Fujiyama, T., Kanda, T., Sato, M., Wang, Z., Ma, J., Nakane, S., Tomita, J., Ikkyu, A., et al. (2016). Forward-genetics analysis of sleep in randomly mutagenized mice. Nature *539*, 378–383.

Halassa, M.M., Florian, C., Fellin, T., Munoz, J.R., Lee, S.Y., Abel, T., Haydon, P.G., and Frank, M.G. (2009). Astrocytic modulation of sleep homeostasis and cognitive consequences of sleep loss. Neuron *61*, 213–219.

Han, K., Holder, J.L., Jr., Schaaf, C.P., Lu, H., Chen, H., Kang, H., Tang, J., Wu, Z., Hao, S., Cheung, S.W., et al. (2013). SHANK3 overexpression causes manic-like behaviour with unique pharmacogenetic properties. Nature *503*, 72–77.

Hayaishi, O., Urade, Y., Eguchi, N., and Huang, Z.L. (2004). Genes for prostaglandin d synthase and receptor as well as adenosine A2A receptor are involved in the homeostatic regulation of nrem sleep. Arch. Ital. Biol. *142*, 533–539.

Hendricks, J.C., Sehgal, A., and Pack, A.I. (2000). The need for a simple animal model to understand sleep. Prog. Neurobiol. *61*, 339–351.

Honda, T., Fujiyama, T., Miyoshi, C., Ikkyu, A., Hotta-Hirashima, N., Kanno, S., Mizuno, S., Sugiyama, F., Takahashi, S., Funato, H., et al. (2018). A single phosphorylation site of SIK3 regulates daily sleep amounts and sleep need in mice. Proc. Natl. Acad. Sci. U S A *115*, 10458.

Jhou, T.C., Fields, H.L., Baxter, M.G., Saper, C.B., and Holland, P.C. (2009a). The rostromedial tegmental nucleus (RMTg), a GABAergic afferent to midbrain dopamine neurons, encodes aversive stimuli and inhibits motor responses. Neuron *61*, 786–800.

Jhou, T.C., Geisler, S., Marinelli, M., Degarmo, B.A., and Zahm, D.S. (2009b). The mesopontine rostromedial tegmental nucleus: a structure targeted by the lateral habenula that projects to the ventral tegmental area of Tsai and substantia nigra compacta. J. Comp. Neurol. *513*, 566–596.

Johnson, S.L. (2005). Mania and dysregulation in goal pursuit: a review. Clin. Psychol. Rev. *25*, 241–262.

Lazarus, M., Oishi, Y., Bjorness, T.E., and Greene, R.W. (2019). Gating and the need for sleep: dissociable effects of adenosine A1 and A2A receptors. Front. Neurosci. *13*, 740.

Leahy, R.L. (1999). Decision making and mania. J. Cogn. Psychother. *13*, 83–105.

Logan, R.W., and McClung, C.A. (2016). Animal models of bipolar mania: the past, present and future. Neuroscience *321*, 163–188.

Lu, J., Jhou, T.C., and Saper, C.B. (2006). Identification of wake-active dopaminergic neurons in the ventral periaqueductal gray matter. J. Neurosci. *26*, 193–202.

Ma, Y., Miracca, G., Yu, X., Harding, E.C., Miao, A., Yustos, R., Vyssotski, A.L., Franks, N.P., and Wisden, W. (2019). Galanin neurons unite sleep homeostasis and alpha2-adrenergic sedation. Curr. Biol. *29*, 3315–3322.e3.

Maddaloni, G., Migliarini, S., Napolitano, F., Giorgi, A., Nazzi, S., Biasci, D., De Felice, A., Gritti, M., Cavaccini, A., Galbusera, A., et al. (2018). Serotonin depletion causes valproate-responsive manic-like condition and increased hippocampal neuroplasticity that are reversed by stress. Sci. Rep. *8*, 11847.

Marangoni, C., De Chiara, L., and Faedda, G.L. (2015). Bipolar disorder and ADHD: comorbidity and diagnostic distinctions. Curr. Psychiatry Rep. *17*, 604.

Naylor, E., Bergmann, B.M., Krauski, K., Zee, P.C., Takahashi, J.S., Vitaterna, M.H., and Turek, F.W. (2000). The circadian clock mutation alters sleep homeostasis in the mouse. J. Neurosci. *20*, 8138.

Oishi, Y., and Lazarus, M. (2017). The control of sleep and wakefulness by mesolimbic dopamine systems. Neurosci. Res. *118*, 66–73.

Oishi, Y., Suzuki, Y., Takahashi, K., Yonezawa, T., Kanda, T., Takata, Y., Cherasse, Y., and Lazarus, M. (2017). Activation of ventral tegmental area dopamine neurons produces wakefulness through dopamine D2-like receptors in mice. Brain Struct. Funct. *222*, 2907–2915.

Oltmanns, T.F. (1978). Selective attention in schizophrenic and manic psychoses: the effect of distraction on information processing. J. Abnorm. Psychol. *87*, 212–225.

Omelchenko, N., and Sesack, S.R. (2009). Ultrastructural analysis of local collaterals of rat ventral tegmental area neurons: GABA phenotype and synapses onto dopamine and GABA cells. Synapse *63*, 895–906.

Palchykova, S., Winsky-Sommerer, R., Meerlo, P., Dürr, R., and Tobler, I. (2006). Sleep deprivation impairs object recognition in mice. Neurobiol. Learn. Mem. *85*, 263–271.

Perry, W., Minassian, A., Paulus, M.P., Young, J.W., Kincaid, M.J., Ferguson, E.J., Henry, B.L., Zhuang, X., Masten, V.L., Sharp, R.F., et al. (2009). A reverse-translational study of dysfunctional exploration in psychiatric disorders: from mice to men. Arch. Gen. Psychiatry *66*, 1072–1080.

Prickaerts, J., Moechars, D., Cryns, K., Lenaerts, I., van Craenendonck, H., Goris, I., Daneels, G., Bouwknecht, J.A., and Steckler, T. (2006). Transgenic mice overexpressing glycogen synthase kinase 3beta: a putative model of hyperactivity and mania. J. Neurosci. *26*, 9022–9029.

Qu, W.M., Huang, Z.L., Xu, X.H., Matsumoto, N., and Urade, Y. (2008). Dopaminergic D1 and D2 receptors are essential for the arousal effect of modafinil. J. Neurosci. *28*, 8462–8469.

Qu, W.M., Xu, X.H., Yan, M.M., Wang, Y.Q., Urade, Y., and Huang, Z.L. (2010). Essential role of dopamine D2 receptor in the maintenance of wakefulness, but not in homeostatic regulation of sleep, in mice. J. Neurosci. *30*, 4382–4389.

Rolls, A., Colas, D., Adamantidis, A., Carter, M., Lanre-Amos, T., Heller, H.C., and de Lecea, L. (2011). Optogenetic disruption of sleep continuity impairs memory consolidation. Proc. Natl. Acad. Sci. U S A *108*, 13305.

Saper, C.B., Scammell, T.E., and Lu, J. (2005). Hypothalamic regulation of sleep and circadian rhythms. Nature *437*, 1257–1263.

Satzer, D., and Bond, D.J. (2016). Mania secondary to focal brain lesions: implications for understanding the functional neuroanatomy of bipolar disorder. Bipolar Disord. *18*, 205–220.

Shen, Y.C., Chen, Y.C., Peng, G.S., and Lin, W.W. (2005). Risperidone - related unilateral rubral tremor in a manic patient—a case report. Tzu Chi Med J. *17*, 437–439.

Shiah, I.S., and Yatham, L.N. (2000). Serotonin in mania and in the mechanism of action of mood stabilizers: a review of clinical studies. Bipolar Disord. *2*, 77–92.

Suzuki, A., Sinton, C.M., Greene, R.W., and Yanagisawa, M. (2013). Behavioral and biochemical dissociation of arousal and homeostatic sleep need influenced by prior wakeful experience in mice. Proc. Natl. Acad. Sci. U S A *110*, 10288–10293.

Takata, Y., Oishi, Y., Zhou, X.Z., Hasegawa, E., Takahashi, K., Cherasse, Y., Sakurai, T., and Lazarus, M. (2018). Sleep and wakefulness are controlled by ventral medial midbrain/pons GABAergic neurons in mice. J. Neurosci. *38*, 10080–10092.

Taylor, N.E., Van Dort, C.J., Kenny, J.D., Pei, J., Guidera, J.A., Vlasov, K.Y., Lee, J.T., Boyden, E.S., Brown, E.N., and Solt, K. (2016). Optogenetic activation of dopamine neurons in the ventral tegmental area induces reanimation from general anesthesia. Proc. Natl. Acad. Sci. U S A *113*, 12826–12831.

Taylor, S.R., Badurek, S., Dileone, R.J., Nashmi, R., Minichiello, L., and Picciotto, M.R. (2014). GABAergic and glutamatergic efferents of the mouse ventral tegmental area. J. Comp. Neurol. *522*, 3308–3334.

van Enkhuizen, J., Henry, B.L., Minassian, A., Perry, W., Milienne-Petiot, M., Higa, K.K., Geyer, M.A., and Young, J.W. (2014). Reduced dopamine transporter functioning induces high-reward risk-preference consistent with bipolar disorder. Neuropsychopharmacology *39*, 3112–3122.

World Health Organization. (2004). ICD-10 : International Statistical Classification of Diseases and Related Health Problems : Tenth Revision (World Health Organization).

Young, J.W., Henry, B.L., and Geyer, M.A. (2011a). Predictive animal models of mania: hits, misses and future directions. Br. J. Pharmacol. *164*, 1263–1284.

Young, J.W., Minassian, A., Paulus, M.P., Geyer, M.A., and Perry, W. (2007). A reverse-translational approach to bipolar disorder: rodent and human studies in the Behavioral Pattern Monitor. Neurosci. Biobehav. Rev. *31*, 882–896.

Young, J.W., van Enkhuizen, J., Winstanley, C.A., and Geyer, M.A. (2011b). Increased risk-taking behavior in dopamine transporter knockdown mice: further support for a mouse model of mania. J. Psychopharmacol. *25*, 934–943.

Yu, X., Li, W., Ma, Y., Tossell, K., Harris, J.J., Harding, E.C., Ba, W., Miracca, G., Wang, D., Li, L., et al. (2019). GABA and glutamate neurons in the VTA regulate sleep and wakefulness. Nat. Neurosci. *22*, 106–119.

iScience, Volume *23*

Supplemental Information

Ablation of Ventral Midbrain/Pons GABA Neurons Induces Mania-like Behaviors with Altered Sleep Homeostasis and Dopamine D_2R-mediated Sleep Reduction

Takato Honda, Yohko Takata, Yoan Cherasse, Seiya Mizuno, Fumihiro Sugiyama, Satoru Takahashi, Hiromasa Funato, Masashi Yanagisawa, Michael Lazarus, and Yo Oishi

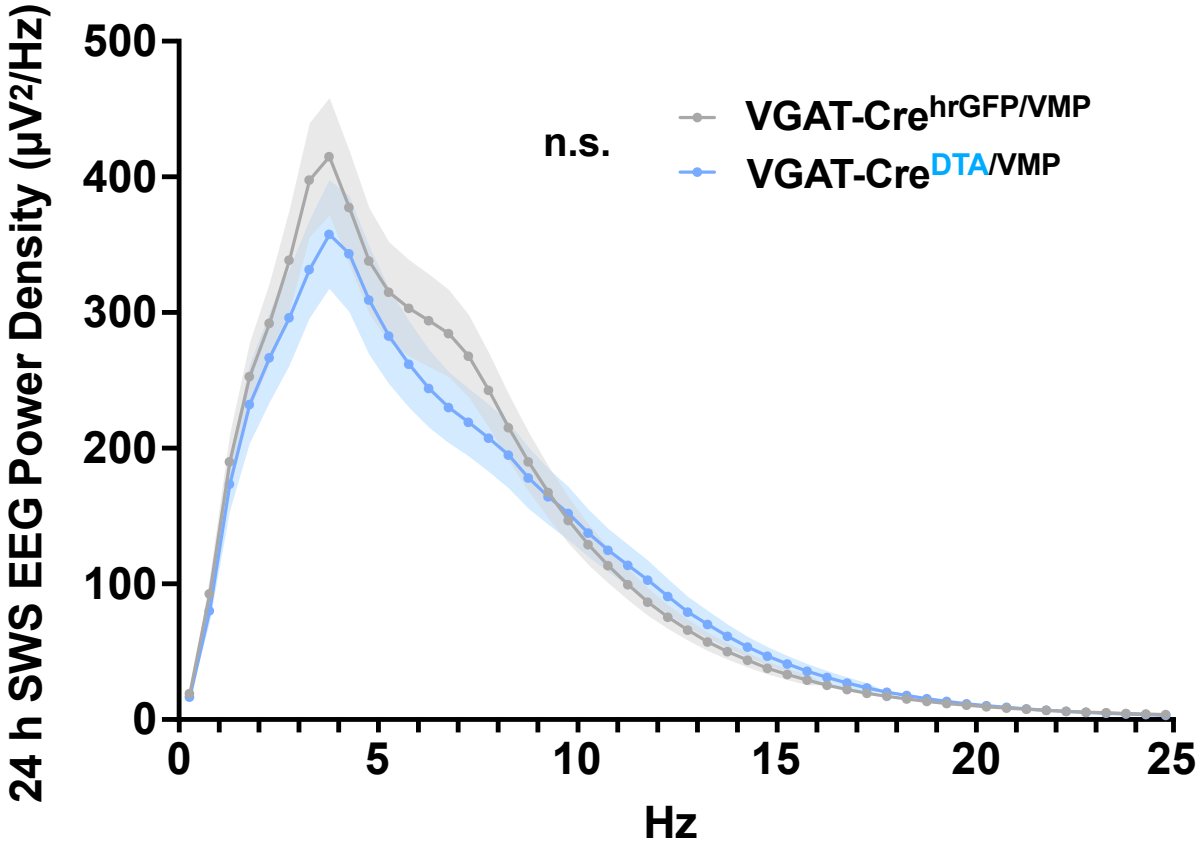

Figure S1. EEG power spectra during 24 h SWS, Related to Figure 2. Two-way repeated measures ANOVA. F (1, 12) = 0.2163, p = 0.6502 (not significant), the main effect of viral transduction. n = 6–8 mice for each group. Data are presented as the mean ± SEM.

TRANSPARENT METHODS

Key Resources Table

REAGENT or RESOURCE	SOURCE	IDENTIFIER
Antibodies		
Rabbit polyclonal anti-D2R	Millipore	AB5084P
Sheep polyclonal anti-Digoxigenin	Roche	11093274910
Bacterial and Virus Strains		
AAV-FLEX-DTA	Takata et al., 2018	N/A
AAV-FLEX-hrGFP	Takata et al., 2018	N/A
Chemicals, Peptides, and Recombinant Proteins		
5-Bromo-4-chloro-3-indolyl phosphate/Nitro blue tetrazolium (BCIP/NBT)	Millipore-Sigma	B1911
Avidin–biotin complex (Vectastain ABC Elite Kit)	Vector Laboratories	PK-6100
Modafinil	Sigma-Aldrich	M6940
Experimental Models: Organisms/Strains		
Mouse: VGAT-Cre	Vong et al., 2011	N/A
Mouse: VGAT-Cre; D_2R KO	This paper	N/A
Mouse: C57BL/6J	The Jackson Laboratory	JAX: 006494
Oligonucleotides		
Primers for VGAT riboprobe Forward: 5'-GCATGTTCGTGCTGGGCCTACC-3' Reverse: 5'-CAGCGCAGCGTCAGCCCCCAG-3' conjugated with the T7 promoter	Takata et al., 2018	N/A
Genotyping Primers for VGAT-Cre; D_2R KO mice Forward: 5'-GAGCCAAAATAATCCCGTCA-3' Reverse: 5'-GCACTGAGCAAGAATGACCA-3'	This paper	N/A
Software and Algorithms		
SMART	Panlab	https://www.panlab.com/en/products/smart-video-tracking-software-panlab
SLEEPSIGN	Kissei Comtec	http://www.sleepsign.com/
GraphPad Prism 7.0	GraphPad Software	https://www.graphpad.com/scientific-software/prism/

Animals

The VGAT-Cre (Vong et al., 2011) (kindly provided by Dr. Bradford Lowell, Harvard Medical School, C57BL/6 and 129 mixed background), VGAT-Cre;D_2R KO (newly generated in this study), and C57BL/6J wild-type (WT; The Jackson Laboratory, used in social interaction test)

mouse strains were used in this study. Male mice (9–27 weeks) used in the behavioral experiments were single-housed in insulated sound-proof chambers maintained at an ambient temperature of 23 ± 0.5°C with 55 ± 3% humidity on a 12 h light/dark cycle (lights on at 8:00). Food and water were provided *ad libitum*. All experiments were performed in accordance with the Animal Care Committee of the University of Tsukuba, and every effort was made to minimize the number of animals used as well as any pain or discomfort.

Surgery

The mice used in the behavioral experiments were anesthetized with isoflurane (4% for induction, 2% for maintenance) for brain microinjection. To selectively ablate GABAergic neurons in the VMP, VGAT-Cre, VGAT-Cre;$D_2R^{-/-}$, or VGAT-Cre;$D_2R^{+/+}$ mice were injected bilaterally into the VMP (3.4 mm posterior and 0.2 mm lateral to bregma, 4.4 mm below the dura) with AAV-FLEX-DTA (Takata et al., 2018) (120 nl, 8.6×10^{10} particles ml^{-1}) or AAV-FLEX-hrGFP (Takata et al., 2018) (120 nl, 1.5×10^{11} particles ml^{-1}) using a glass micropipette and an air pressure injector system. For monitoring sleep/wake behavior, the mice were chronically implanted with electroencephalography (EEG) and electromyography (EMG) electrodes for polysomnography (Oishi et al., 2016). As EEG electrodes, two stainless steel screws were implanted into the skull. As EMG electrodes, two insulated Teflon-coated silver wires were placed bilaterally into the trapezius muscles. The electrodes were fixed to the skull using dental acrylic.

Histology

For histologic analyses, the mice were deeply anesthetized with an overdose of chloral hydrate (500 mg/kg, i.p.) and perfused through the left ventricle of the heart with saline, followed by neutral buffered 10% formalin. The brains were removed and placed in 20% sucrose in phosphate-buffered saline overnight at 4°C to reduce freezing artifacts. The brains were then

sectioned at 40 μm on a freezing microtome. For in situ hybridization, a 918-bp digoxigenin-labeled riboprobe for VGAT mRNA was generated by PCR amplification with the forward (5'-GCATGTTCGTGCTGGGCCTACC-3') and reverse (5'-CAGCGCAGCGTCAGCCCCCAG-3') primers conjugated with the T7 promoter using mouse tail genomic DNA (gDNA) as a template, followed by in vitro transcription. The brain sections were then incubated with a 1 μg ml^{-1} of the VGAT probe in 5× sodium citrate buffer containing 50% formamide at 50°C overnight, washed in 1× saline sodium citrate buffer at 50°C, incubated with alkaline phosphatase-conjugated anti-digoxigenin antibody (1:500, Roche) overnight, and visualized by reaction with 5-bromo-4-chloro-3-indolyl phosphate/nitro blue tetrazolium (BCIP/NBT, Millipore). Immunohistochemistry for D_2R was performed on free-floating sections, the brain sections were incubated in 0.3% hydrogen peroxide for 30 min and then for two nights at 4°C and one night at room temperature with a rabbit anti-D_2R antibody (1:500; Millipore). Sections were then treated with avidin–biotin complex (1:1000; Vectastain ABC Elite kit; Vector Laboratories) for 1 h, and immunoreactive cells were visualized by reaction with 3,3'-diaminobenzidine, 0.01% nickel ammonium sulfate, 0.005% cobalt chloride, and 0.1% hydrogen peroxide.

Behavioral experiments

During the entire behavioral testing period, the mice were single-housed in insulated sound-proof chambers, and each cage was visually isolated with partitions. The cages were changed weekly. Only male mice were used in the behavioral experiments. The mice were handled for 2 min twice a day for 3 days total prior to the behavioral experiments. All behavioral assays were performed during the light period (8:00-20:00) except the EEG/EMG recordings, which required 24 h data sampling. The behavioral room was maintained at 23.5 ± 2.0°C with 55 ± 10% humidity. During the behavioral tests, white noise was constantly generated in the room. Before and after each individual test, all the apparatuses were sterilized with weak acidic water.

The behavioral test battery (Figures 1 and 4) was performed in the following order with at least a 6-day interval between tasks: nest building, open field, social interaction, elevated plus maze, novel object recognition, Y-maze, tail suspension, and forced swim. Different groups of mice were used for the EEG/EMG recording (Figures 2 and 4) to avoid the effect of EEG/EMG wire implantation on other behavioral tests.

Open field test

The open field test was performed according to the previously described procedures (Crawley, 2007; Seibenhener and Wooten, 2015) with minor modifications. The mice were individually placed in a white plastic box (40 cm wide × 40 cm high × 40 cm deep). The light level at the center of the box was adjusted to 100–130 lux. Spontaneous locomotor activity was recorded using a video camera. Total distance traveled (m) during the 10-min period was analyzed automatically using video tracking software (SMART, Panlab).

Tail suspension test

The tail suspension test was performed according to the previously described procedures (Can et al., 2012; Crawley, 2007) with minor modifications. A transparent plastic hollow cylinder (4 cm long, 4 mm diameter) was placed around the mouse tail to prevent climbing behavior. The mice were placed individually in a lane of a plastic tail suspension apparatus comprising four lanes (each lane: 15 cm wide, 60 cm high), and each lane was visually isolated from the others by opaque walls. The mice were suspended 30 cm above the floor, using a 15-cm piece of adhesive tape attached 1 cm from the tip of the tail. Immobility (s) during the 6-min period was manually analyzed. Immobility was defined as the absence of active movements, including shaking of the body and running-like motions using all four legs.

Forced swim test

A forced swim test was performed according to the previously described procedures (Crawley, 2007; Yankelevitch-Yahav et al., 2015) with minor modifications. The mice were placed individually in a plastic chamber (23 cm high × 20 cm diameter) filled with water (23.5 ± 2.0ºC, 15 cm deep), and spontaneous activity was recorded using a video camera. Immobility (s) during the last 4 min of the recorded 6-min period was manually analyzed. Immobility was defined as the absence of movements except minimal motions required to keep the head above water.

Sociability and social interaction test

The social interaction test was performed according to the previously described procedures (Crawley, 2007; Moy et al., 2004) with some modifications. An unfamiliar mouse (C57BL/6J, same age and same sex as the subject mouse) that had no prior contact with the subject mouse, was placed in a transparent plastic chamber (15 cm high × 7 cm diameter containing a band of small holes up to 4 cm from the bottom, which allows the mice to make nose contact) and set in one corner of a plastic white box (40 cm wide × 40 cm high × 40 cm deep). An empty identical chamber was set in the diagonally opposite corner. The subject mouse was then individually placed in one corner of the box where no chambers were set. The light level at the center of the box was adjusted to 100–130 lux. Spontaneous activity was recorded using a video camera. The ratio (%) of time spent in the zone surrounding the unfamiliar mouse chamber to the time spent in both zones surrounding empty and unfamiliar mouse champers during the 10-min period was analyzed automatically using video tracking software (SMART, Panlab).

Elevated plus maze

The elevated plus maze task was performed based on the previous studies (Crawley, 2007; Komada et al., 2008) with minor modifications. A gray plastic plus-maze comprising two open

arms (5 cm wide × 30 cm long) and two closed arms (5 cm wide × 30 cm long with 20 cm high walls) was elevated 50 cm above the floor. The light level was adjusted to 150–170 lux for the open arms and 10–20 lux for the closed arms. The mice were set on the center of plus-maze, and their spontaneous activity was recorded using a video camera. The time spent in the center was also counted as the time in the open arms. The ratio (%) of time spent in the open arms to the time spent in the entire area during the 5-min period was manually analyzed.

Nest building

Mice were placed in new individual cages, each containing a single square piece of pressed cotton (5 × 5 cm, 2.5 g, Nestlets, Ancare). Nest building score was evaluated 1 h later based on the previously described five-point scale criteria (Deacon, 2006; Eban-Rothschild et al., 2016).

Novel object recognition

The novel object recognition test was performed as previously described (Leger et al., 2013) with minor modifications. Two different objects (object A: Falcon tissue culture flask filled with sand: 10 cm high × 4 cm wide × 2.5 cm deep, object B: Lego brick tower: 10 cm high × 3 cm wide × 3 cm deep) were prepared. On Day 1 as a familiarization session, two identical copies of object A were each set in the center of opposite quadrants of a white plastic box (40 cm wide × 40 cm high × 40 cm deep). The mice were placed individually in one of the corners where no objects were placed and exposed to object A for a 10-min period as familiarization. The light level at the center of the box was adjusted to 100–130 lux. Spontaneous activity was recorded using a video camera. After the 24-h interval, on Day 2 as a test session, one of the copies of object A was replaced by object B as a novel object for the mice. The ratio (%) of time spent in the familiar/novel object zone to the time spent in both zones during the 10-min period was analyzed automatically using video tracking software (SMART, Panlab).

Y maze

The Y-maze task was performed according to the procedures described previously (Miedel et al., 2017; Sarnyai et al., 2000) with minor modifications. The mice were individually placed in one arm of the gray plastic Y-shaped maze comprising three arms (3 cm wide × 38 cm long, 12 cm high angled walls), facing the center, and spontaneous activity was recorded using a video camera. The number of entries into each arm and the spontaneous alternation rate during the 10-min period was manually analyzed. When all four legs of the mouse entered an arm, it was counted as an arm entrance. The spontaneous alternation rate (%) was calculated using the following formula.

$$\text{Spontaneous alternation (\%)} = \frac{\text{Number of 3 consecutive entries to different arms}}{\text{Total number of arm entries - 2}} \times 100$$

EEG/EMG recordings

EEG/EMG recordings were performed based on the previous study (Oishi et al., 2016). Briefly, after allowing 1–2 weeks for postoperative recovery and transgene expression, the mice were connected with EEG/EMG recording cables. The EEG/EMG signals were amplified and filtered by an amplifier (Biotex; EEG: 0.5–64 Hz, EMG: 16–64 Hz), digitized at a sampling rate of 128 Hz, and recorded using SLEEPSIGN software (Kissei Comtec). Vigilance states were scored offline by characterizing 10-s epochs into three stages: awake, SWS, and REMS according to standard criteria (Oishi et al., 2016). Sleep latency after SD was defined as the time from the end of SD to the appearance of the first SWS episode lasting longer than 30 s. Delta power (%) was calculated based on the ratio of delta (0.5–4.0 Hz) frequency EEG power to the total (0–25.0 Hz) EEG power during SWS (Figure 2C). Although VGAT-Cre$^{DTA/VMP}$ mice took time to exhibit the first SWS episode after SD (Figure 2E), once they were into SWS episodes, the delta power was calculated for every 10-min SWS (not necessary to be a single continuous SWS episode) and the averaged values (across animals) for every 10-min SWS

period after SD were used in Figure 2F. For pharmacologic experiments, modafinil (MilliporeSigma) was dissolved in saline containing 10% DMSO and 2% (w/v) cremophor immediately before use. After baseline recordings for 24 h, VGAT-Cre;$D_2R^{-/-}$ or VGAT-Cre;$D_2R^{+/+}$ mice were intraperitoneally injected with vehicle or modafinil (45 mg/kg).

Generation of VGAT-Cre;D_2R KO mice by the CRISPR/Cas9 system

For generation of the CRISPR-engineered VGAT-Cre;D_2R KO mice with the electroporation method, guide RNA (gRNA), donor single-stranded oligodeoxynucleotide (ssODN), Cas9 protein (Thermo Fisher Scientific), and fertilized eggs of homozygous VGAT-Cre mice were used. The gRNA (5'-GACATTGTTTTATCTCCAGG-3') containing the splicing acceptor (SA) site located across intron 2 and exon 3 of the *D_2R* gene was synthesized using a GeneArt Precision gRNA Synthesis Kit (Thermo Fisher Scientific). The donor ssODN was designed to induce a deletion of the SA site to knockout the *D_2R* gene with the production of a stop codon at exon 4. The 120-bp ssODN was synthesized (Integrated DNA Technologies) with deletion of the SA site (encoded as GG) in the center and two 60-nucleotide arms at the 5‘ and 3‘ ends. Female homozygous VGAT-Cre mice were injected with pregnant mare serum gonadotropin and human chorionic gonadotropin at a 48-h interval. Fertilized one-cell embryos were collected from the oviducts. gRNA, ssODN, and Cas9 protein were introduced into the pronuclei of these one-cell embryos using the electroporator (NEPA21, Nepa Gene). These one-cell embryos were then transferred into pseudopregnant ICR mice for F0 mouse production. Direct sequencing from the gDNA of F0 mice was performed to check SA site deletion. For later genotyping, the gDNA was amplified the forward (5'-GAGCCAAAATAATCCCGTCA-3'), and the reverse (5'-GCACTGAGCAAGAATGACCA-3') primers, and the PCR products (D_2R KO: 361 bp, WT: 363 bp) were digested with NcoI enzyme. Because SA site deletion resulted in the production of a NcoI site, the PCR products of the D_2R KO allele were digested into 201-bp and 160-bp fragments whereas the WT allele was detected as a 363-bp product.

The obtained F0 VGAT-Cre;D_2R KO mice were mated with homozygous VGAT-Cre mice for the F1 production of heterozygous VGAT-Cre;D_2R KO mice. These heterozygous VGAT-Cre;D_2R KO mice were maintained in colonies and mated to produce homozygous VGAT-Cre;D_2R KO mice and littermate WT mice for behavioral experiments

Quantification and statistical analysis

Statistical analysis was performed using Graph Pad Prism 7.0 (GraphPad Software). All data were subjected to D'Agostino–Pearson (Omnibus K2) and Shapiro-Wilk normality tests for Gaussian distribution and variance. For the dataset showing a Gaussian distribution ($p > 0.05$ in normality test), we performed parametric tests such as two-tailed unpaired/paired t test and ANOVA followed by Sidak's multiple comparisons. For datasets that failed to show a Gaussian distribution, we performed a nonparametric test, such as the Mann-Whitney U test. Significance levels in the figures are represented as *$p < 0.05$, **$p < 0.01$, ***$p < 0.001$, and ****$p < 0.0001$. Error bars in the graphs represent mean ± SEM.

Supplemental References

Can, A., Dao, D.T., Terrillion, C.E., Piantadosi, S.C., Bhat, S., and Gould, T.D. (2012). The tail suspension test. J. Vis. Exp. *59*, e3769.

Crawley, J.N. (2007). What's wrong with my mouse? Behavioral phenotyping of transgenic and knockout mice, Second Edition (John Wiley & Sons Inc).

Deacon, R.M. (2006). Assessing nest building in mice. Nat. Protoc. *1*, 1117-1119.

Eban-Rothschild, A., Rothschild, G., Giardino, W.J., Jones, J.R., and de Lecea, L. (2016). VTA dopaminergic neurons regulate ethologically relevant sleep-wake behaviors. Nat. Neurosci. *19*, 1356-1366.

Komada, M., Takao, K., and Miyakawa, T. (2008). Elevated Plus Maze for Mice. J. Vis. Exp. *22*, e1088.

Leger, M., Quiedeville, A., Bouet, V., Haelewyn, B., Boulouard, M., Schumann-Bard, P., and Freret, T. (2013). Object recognition test in mice. Nat. Protoc. *8*, 2531-2537.

Miedel, C.J., Patton, J.M., Miedel, A.N., Miedel, E.S., and Levenson, J.M. (2017). Assessment of Spontaneous Alternation, Novel Object Recognition and Limb Clasping in Transgenic Mouse Models of Amyloid-beta and Tau Neuropathology. J. Vis. Exp. *123*, e55523.

Moy, S.S., Nadler, J.J., Perez, A., Barbaro, R.P., Johns, J.M., Magnuson, T.R., Piven, J., and Crawley, J.N. (2004). Sociability and preference for social novelty in five inbred strains: an approach to assess autistic-like behavior in mice. Genes Brain Behav. *3*, 287-302.

Oishi, Y., Takata, Y., Taguchi, Y., Kohtoh, S., Urade, Y., and Lazarus, M. (2016). Polygraphic Recording Procedure for Measuring Sleep in Mice. J. Vis. Exp. *107*, e53678.

Sarnyai, Z., Sibille, E.L., Pavlides, C., Fenster, R.J., McEwen, B.S., and Toth, M. (2000). Impaired hippocampal-dependent learning and functional abnormalities in the hippocampus in mice lacking serotonin(1A) receptors. Proc. Natl. Acad. Sci. U S A *97*, 14731-14736.

Seibenhener, M.L., and Wooten, M.C. (2015). Use of the Open Field Maze to measure locomotor and anxiety-like behavior in mice. J. Vis. Exp. *96*, e52434.

Takata, Y., Oishi, Y., Zhou, X.Z., Hasegawa, E., Takahashi, K., Cherasse, Y., Sakurai, T., and Lazarus, M. (2018). Sleep and Wakefulness Are Controlled by Ventral Medial Midbrain/Pons GABAergic Neurons in Mice. J. Neurosci. *38*, 10080-10092.

Vong, L., Ye, C., Yang, Z., Choi, B., Chua, S., Jr., and Lowell, B.B. (2011). Leptin action on GABAergic neurons prevents obesity and reduces inhibitory tone to POMC neurons. Neuron *71*, 142-154.

Yankelevitch-Yahav, R., Franko, M., Huly, A., and Doron, R. (2015). The forced swim test as a model of depressive-like behavior. J. Vis. Exp. *97*, e52587.